# 1 Supplementary material

Figures 1 and 2 present the improvement of the $p(D^0)$ and $\eta(D^0)$ distributions following both kinematic matching and weighting procedures. Figures 3 and 4 show the results of the measurements of the analysis with data and simulation, respectively. Figures 5 and 6 present the improvement of $p(D^0)$, $\eta(D^0)$ and $R^{KK}(t)$ following the kinematic matching procedure with fast simulation. Figure 7 presents the measurement of $y_{CP}^{CC}$ with the full Run 2 data set. Figure 8 shows the updated world average value of $y_{CP} - y_{CP}^{K\pi}$. Figures 9, 10, 11 and 12 display the improvement of charm mixing parameters with the measurement of this paper.

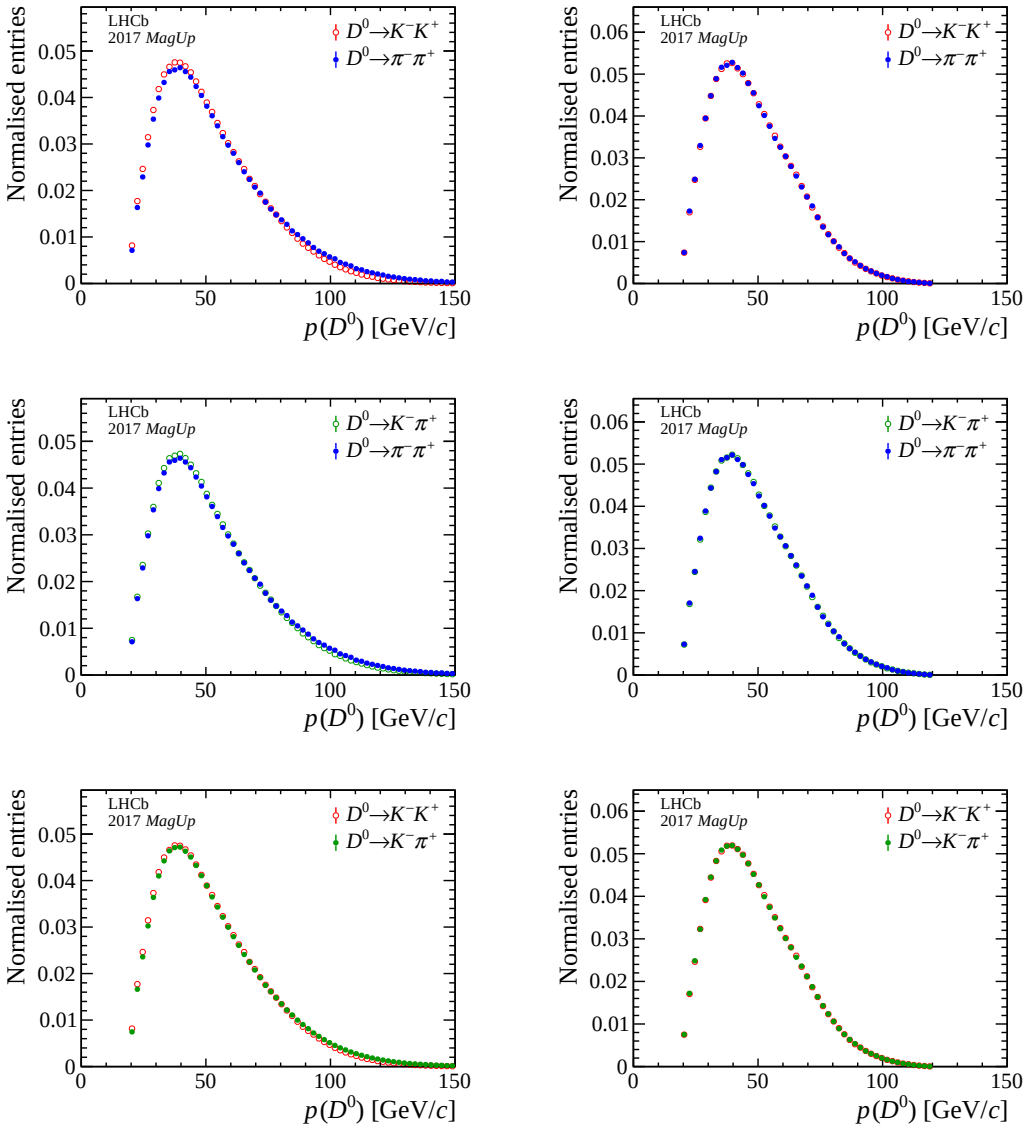


Figure 1: (Left) normalised distributions of the $D^0$ momentum in the raw condition, and (right) following both kinematic matching and weighting procedures. The distributions are shown for the (top) $y_{CP}^{CC}$, (middle) $y_{CP}^{\pi\pi} - y_{CP}^{K\pi}$ and (bottom) $y_{CP}^{KK} - y_{CP}^{K\pi}$ measurements. The plots are obtained with the 2017 *MagUp* sample.

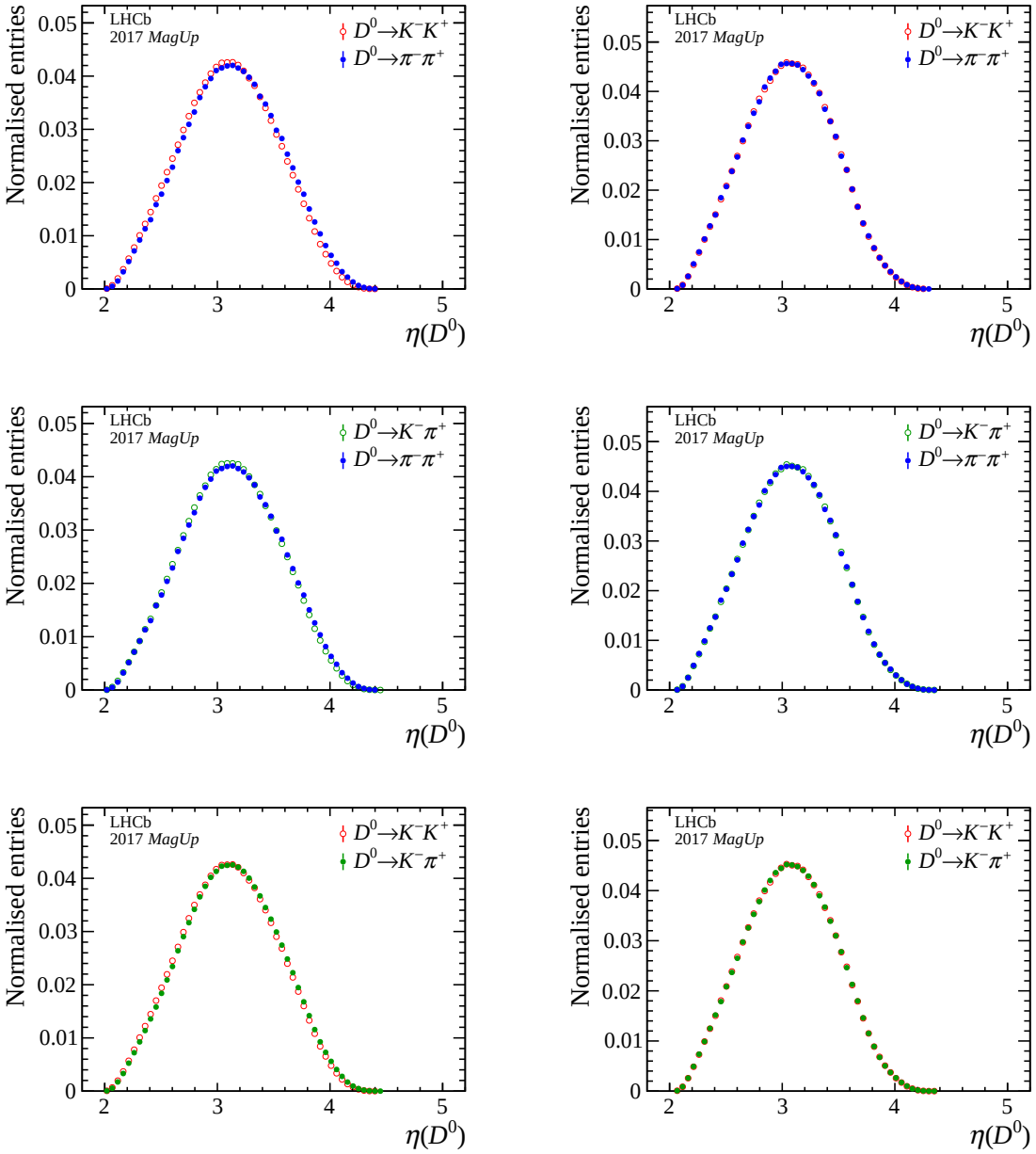


Figure 2: (Left) normalised distributions of the $D^0$ pseudorapidity in the raw condition, and (right) following both kinematic matching and weighting procedures. The distributions are shown for the (top) $y_{CP}^{CC}$, (middle) $y_{CP}^{\pi\pi} - y_{CP}^{K\pi}$ and (bottom) $y_{CP}^{KK} - y_{CP}^{K\pi}$ measurements. The plots are obtained with the 2017 *MagUp* sample.

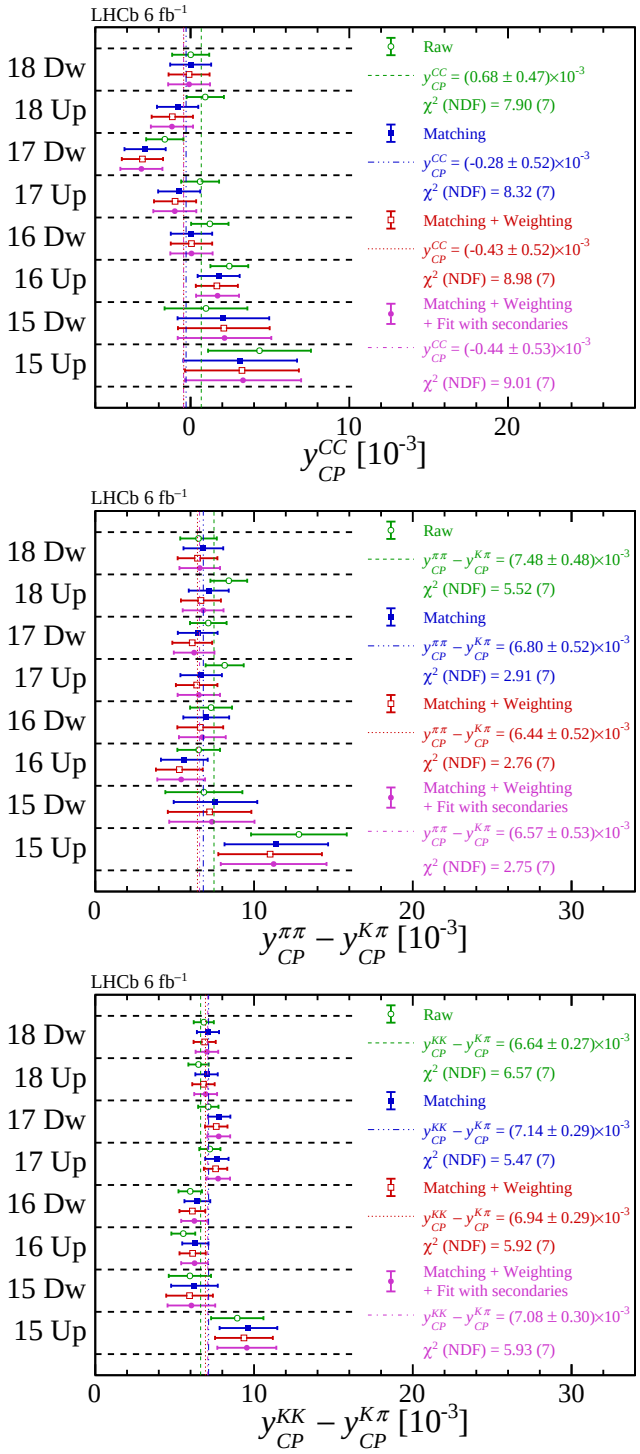


Figure 3: Results for (top) $y_{CP}^{CC}$, (centre) $y_{CP}^{\pi\pi} - y_{CP}^{K\pi}$ and (bottom) $y_{CP}^{KK} - y_{CP}^{K\pi}$. The measurements employing raw data, and following the kinematic matching and both matching and weighting conditions are shown in green, blue and red, respectively, and are obtained by fitting with an exponential model. The measurements in purple employ the fit model of where the presence of secondary decays is considered. In the y-axis labels, the data-taking year is abbreviated with the last two digits only and the magnet polarity *MagUp* (*MagDown*) is abbreviated as "Up" ("Dw"). The results for each condition on the right side of each plot are weighted averages, $\chi^2$ and numbers of degrees of freedom (NDF) determined from a constant $\chi^2$ fit to each individual value. The uncertainties are only statistical.

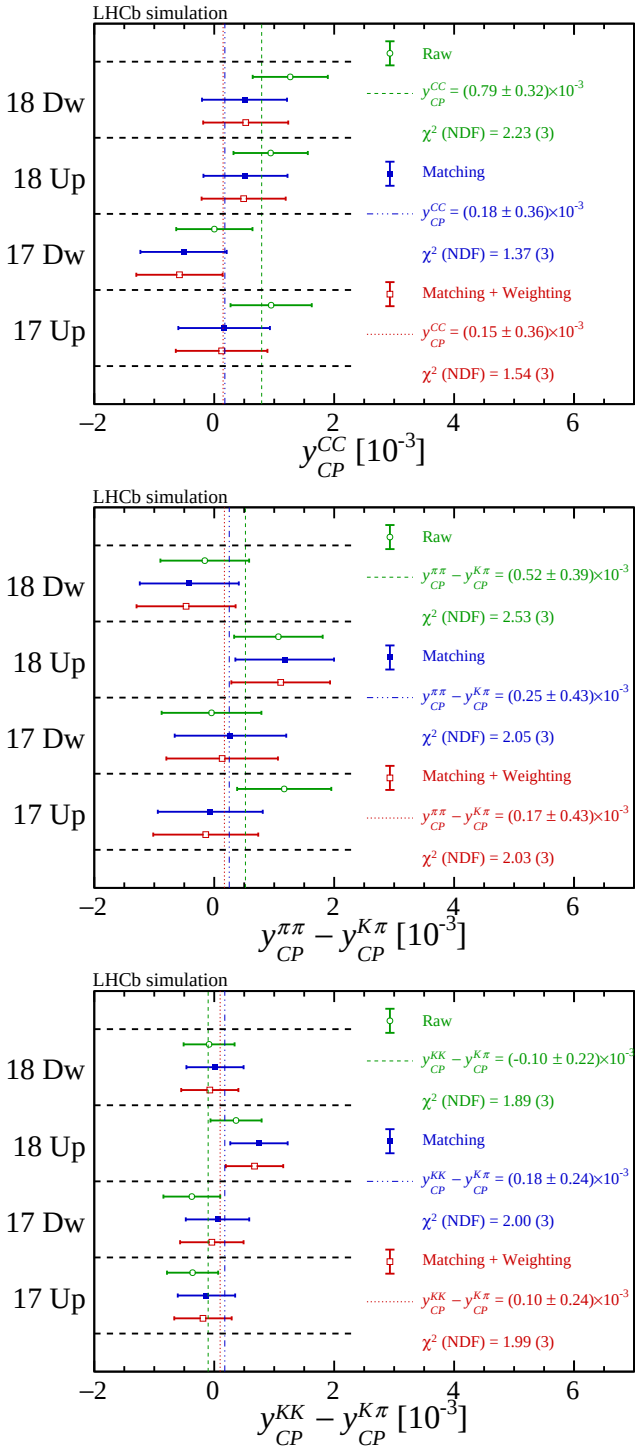


Figure 4: Results for (top) $y_{CP}^{CC}$, (centre) $y_{CP}^{\pi\pi} - y_{CP}^{K\pi}$ and (bottom) $y_{CP}^{KK} - y_{CP}^{K\pi}$, obtained with simulation. The measurements under the raw condition, and following the kinematic matching and both kinematic and reweighting conditions are shown in green, blue and red, respectively, and are obtained by fitting with an exponential model. The uncertainties are only statistical.

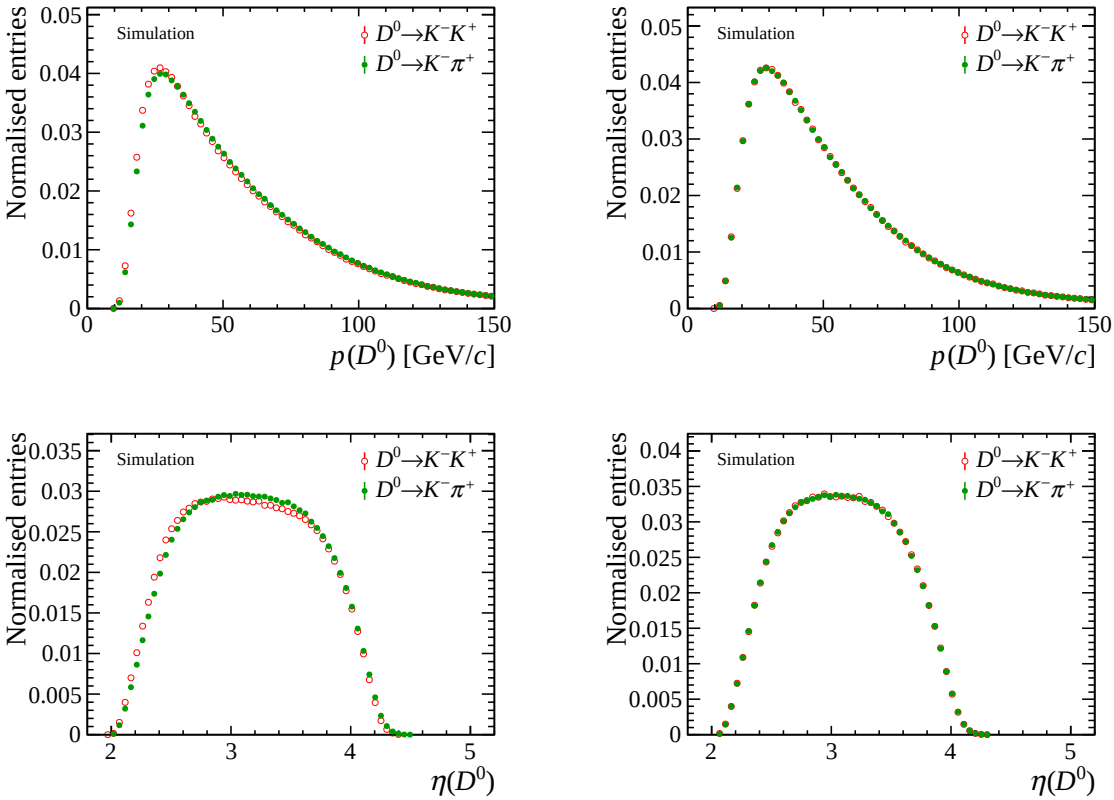


Figure 5: (Left) normalised distributions of the $D^0$ (top) momentum and (bottom) pseudorapidity in the raw condition, and (right) following the kinematic matching procedure. The plots are obtained with fast simulation.

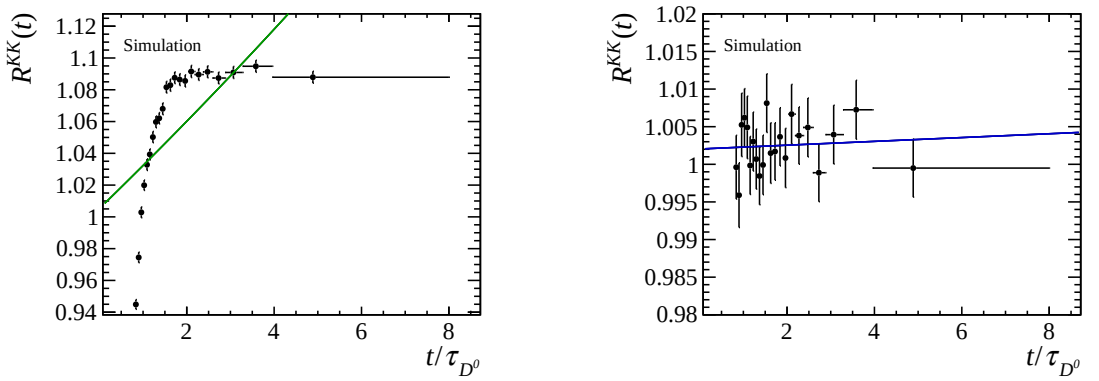


Figure 6: Decay-time ratios $R^{KK}(t)$ (left) in the raw condition and (right) following the kinematic matching procedure. The solid lines correspond to fits performed to determine $y_{CP}^{KK} - y_{CP}^{K\pi}$. The plots are obtained with fast simulation.

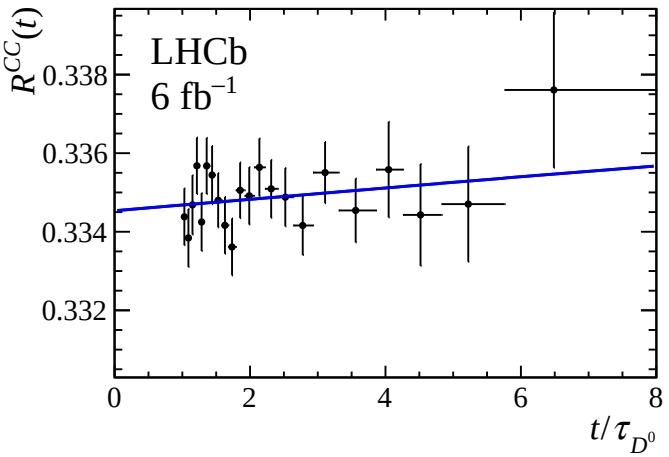


Figure 7: Distribution of $R^{CC}(t)$ using the full LHCb Run 2 data set, with the result of $y_{CP}^{CC}$ overlaid in blue.

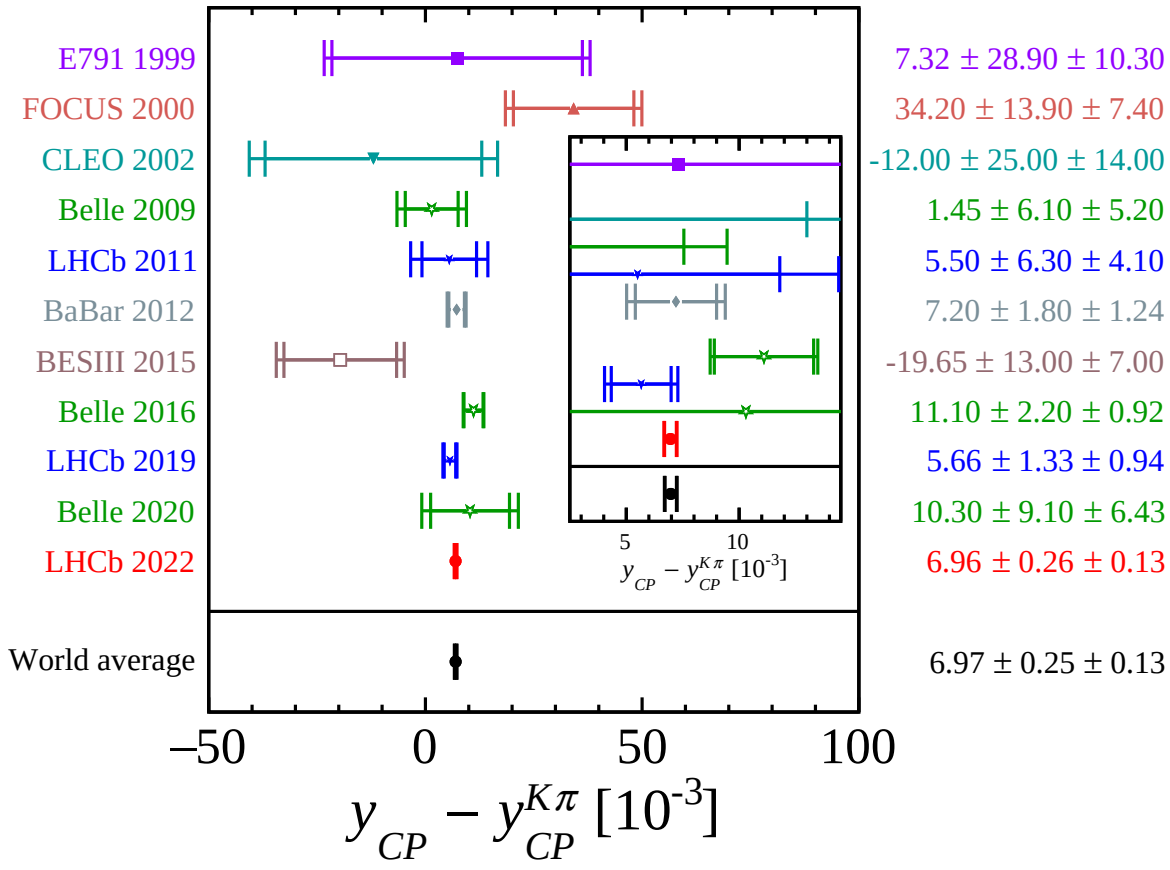


Figure 8: Updated world average value of $y_{CP} - y_{CP}^{K\pi}$ [1–10]. The first uncertainties are statistical and the second systematic. The measurement of this paper is denoted as *LHCb 2021*. The inset plot shows the measurements in a reduced horizontal range and with a compressed vertical scale. The $\chi^2$/NDF value of the world average fit is measured as 10.9/10, corresponding to a probability of 36.3%.

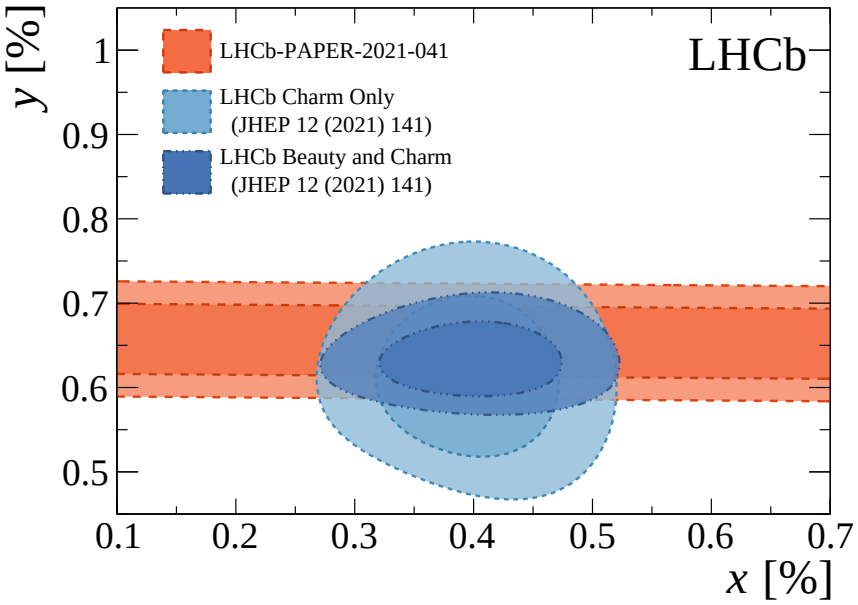


Figure 9: Profile likelihood contours of $y$ versus $x \equiv (m_1 - m_2)/\Gamma$ of the (light blue) LHCb Charm Only and (dark blue) LHCb Beauty and Charm combinations [11], and of (red) the measurement of this paper. In the latter, $x_D$ is fixed to the global best fit, where one can see that the improvements on $y$ from this measurement and the Beauty and Charm combinations are compatible and similar in size. The contours indicate the 68% and 95% confidence region.

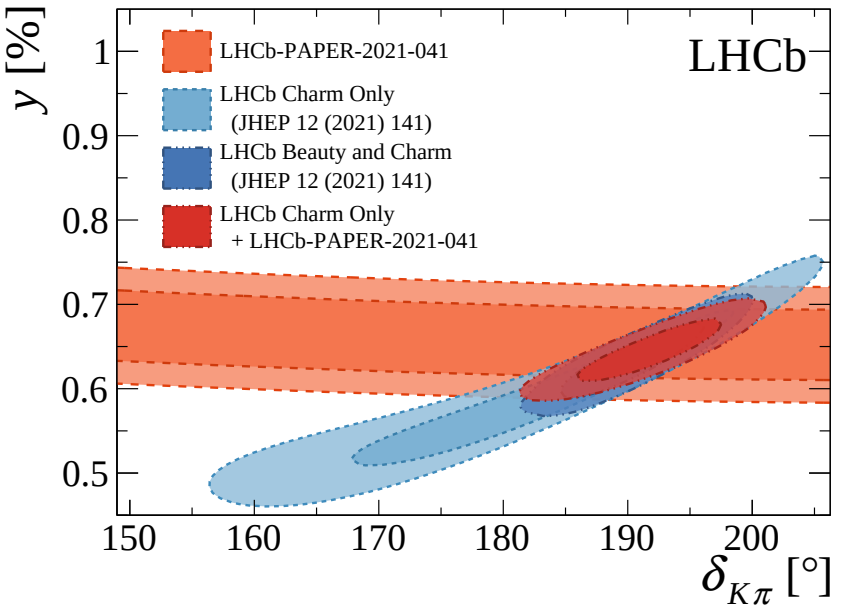


Figure 10: Profile likelihood contours of $y$ versus $\delta_{K\pi}$. The combination of (red) LHCb Charm Only results with the measurement of this paper is compared to (dark blue) the LHCb Beauty and Charm combination [11], indicating similar improvements with respect to (light blue) the LHCb Charm Only combination. The orange band is produced fixing $x_D$ and $R_D$ to the global best fit.

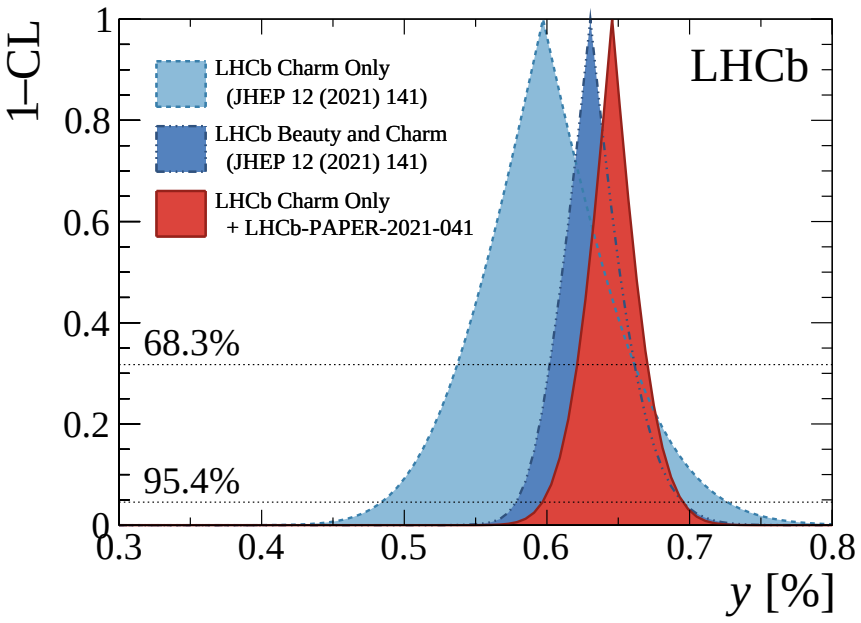


Figure 11: One dimensional $1-\mathrm{CL}$ profiles of $y$ as for the (light blue) LHCb Charm Only and (dark blue) LHCb Beauty and Charm combinations [11], and for (red) the Charm Only combination including the measurement of this paper.

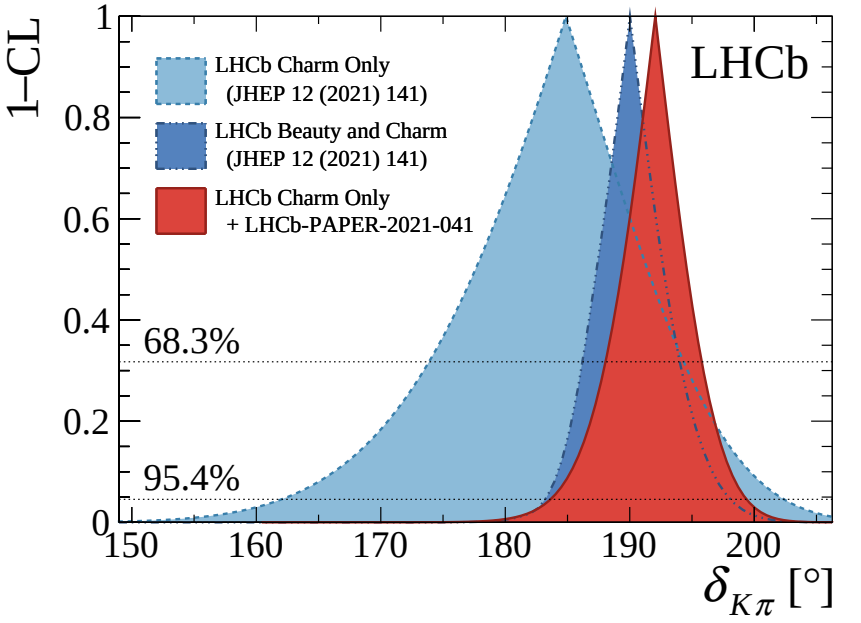


Figure 12: One dimensional $1-\mathrm{CL}$ profiles of $\delta_{K\pi}$ as for the (light blue) LHCb Charm Only and (dark blue) LHCb Beauty and Charm combinations [11], and for (red) the Charm Only combination including the measurement of this paper.

# References


[1] E791 collaboration, E. M. Aitala *et al.*, *Measurements of lifetimes and a limit on the lifetime difference in the neutral D-meson system*, Phys. Rev. Lett. **83** (1999) 32, arXiv:hep-ex/9903012.

[2] FOCUS collaboration, J. M. Link *et al.*, *A Measurement of lifetime differences in the neutral D-meson system*, Phys. Lett. **B485** (2000) 62, arXiv:hep-ex/0004034.

[3] CLEO collaboration, S. E. Csorna *et al.*, *Lifetime differences, direct CP violation and partial widths in $D^0$ meson decays to $K^+K^-$ and $\pi^+\pi^-$*, Phys. Rev. **D65** (2002) 092001, arXiv:hep-ex/0111024.

[4] Belle collaboration, A. Zupanc *et al.*, *Measurement of $y_{CP}$ in $D^0$ meson decays to the $K^0_S K^+ K^-$ final state*, Phys. Rev. **D80** (2009) 052006, arXiv:0905.4185.

[5] LHCb collaboration, R. Aaij *et al.*, *Measurement of mixing and CP violation parameters in two-body charm decays*, JHEP **04** (2012) 129, arXiv:1112.4698.

[6] BaBar collaboration, J. P. Lees *et al.*, *Measurement of $D^0$–$\overline{D}^0$ mixing and CP violation in two-body $D^0$ decays*, Phys. Rev. **D87** (2013) 012004, arXiv:1209.3896.

[7] BESIII collaboration, M. Ablikim *et al.*, *Measurement of $y_{CP}$ in $D^0$–$\overline{D}^0$ oscillation using quantum correlations in $e^+e^- \to D^0\overline{D}^0$ at $\sqrt{s}$ = 3.773 GeV*, Phys. Lett. **B744** (2015) 339, arXiv:1501.01378.

[8] Belle collaboration, M. Starič *et al.*, *Measurement of $D^0$–$\overline{D}^0$ mixing and search for CP violation in $D^0 \to K^+K^-, \pi^+\pi^-$ decays with the full Belle data set*, Phys. Lett. **B753** (2016) 412, arXiv:1509.08266.

[9] LHCb collaboration, R. Aaij *et al.*, *Measurement of the charm-mixing parameter $y_{CP}$*, Phys. Rev. Lett. **122** (2019) 011802, arXiv:1810.06874.

[10] Belle collaboration, M. Nayak *et al.*, *Measurement of the charm-mixing parameter $y_{CP}$ in $D^0 \to K^0_S\omega$ decays at Belle*, Phys. Rev. **D102** (2020) 071102, arXiv:1912.10912.

[11] LHCb collaboration, R. Aaij *et al.*, *Simultaneous determination of CKM angle $\gamma$ and charm mixing parameters*, JHEP **12** (2021) 141, arXiv:2110.02350.